Journal of Applied Polymer Science

Anomalous Impact Strength for Layered Double Hydroxide-Palmitate/Poly(ε-caprolactone) Nanocomposites

Lumbidzani Moyo, Edwin Makhado, and Suprakas Sinha Ray
DST/CSIR National Centre of Nanostructured Materials, Council for Scientific and Industrial Research, Pretoria 0001, South Africa
Correspondence to: S. S. Ray (E-mail: rsuprakas@csir.co.za)

ABSTRACT: Inherent physical properties and commercial availability makes poly(ε-caprolactone) (PCL) very attractive as a potential substitute material for nondegradable polymers for commodity applications. However, a balance of toughness and stiffness is needed in order to transfer this potential into reality, particularly for short-term packaging applications. In this context, layered double hydroxide modified with palmitic acid (LDH-palmitate), was used as a nanoadditive to enhance the mechanical properties of PCL. Composites from PCL were prepared by melt-blending with LDH-palmitate loadings in the 1−10 wt % range. Scanning electron microscopy, transmission electron microscopy, and X-ray diffraction were used to study the structure and morphology of the composites. The results showed homogeneous dispersion of clay particles in composites, but the degree of stacking of clay platelets was related to the LDH-palmitate loadings. Charpy impact test measurements revealed an anomalous toughness improvement in the case of composite containing 5 wt % LDH-palmitate, attributed to a combination of microcavitation and changes in crystallite sizes in the composite. The addition of LDH-palmitate improved the water vapor barrier permeation of neat PCL film. In summary, LDH-palmitate was shown to have potential as a nanoadditive to obtain tougher LDH-PCL composite with improved barrier property. © 2014 Wiley Periodicals, Inc. J. Appl. Polym. Sci. **2014**, *131*, 41109.

KEYWORDS: clay; composites; crystallization; mechanical properties; plasticizer

Received 16 January 2014; accepted 6 June 2014
DOI: 10.1002/app.41109

INTRODUCTION

Toughness of a polymer material is one of the most important selection criteria for many applications. It reflects the degree of energy absorption of a material from the beginning of mechanical load to final fracture.[1] The ability of a polymer to exhibit plastic deformation and resistance to impact without failure is a very desirable attribute.[2] The use of rigid fillers as toughening agents has been suggested to mimic rubber toughening. The advantage of such fillers is that they also improve elastic stiffness of the overall composite. A wide range of fillers have been used in the preparation of nanocomposites such as clays,[3] carbon nanotubes,[4] polyhedral oligomeric silsesquioxanes (POSS),[5] layered double hydroxides (LDHs),[6] expandable graphite,[7] inorganic nanoparticles,[8] and natural fibres.[9]

The improved and value added properties in polymer nanocomposites are envisaged to originate from the interaction of the polymer and filler at the interface. The interfacial region has also been referred to as a "communication bridge" between the filler and matrix; and is conventionally ascribed properties different from those of the bulk matrix because of its proximity to the surface of the filler.[10] During mechanical loading the filler acts as stress concentrations due to the different elastic properties to the polymer. This ultimately leads to a buildup of triaxial stress around the filler particles leading to debonding at the particle-polymer interface. Debonding results in the creation of free volume at a submicron level, this is similar to microcavitation of rubber toughened systems. Zuiderduin et al.[11] demonstrated this phenomenon by toughening polypropylene with $CaCO_3$ nanoparticles. Their notched Izod fracture energy increased from 2 to 40–50 kJ/m^2. The prerequisites for toughness enhancement include small particle size (<5 μm), an aspect ratio of close to unity, filler particles must debond prior to the yield strain of the polymer and the particles should be homogeneously dispersed. However, toughness enhancement is not widely reported for clay filled polymer nanocomposites.[12] In fact some studies revealed that addition of mineral fillers has an embrittling effect on semicrystalline polymer matrices.[13] Given that clays are readily available, their low cost and improvements introduced in many composites (stiffness, strength, and resistance to permeation of gases and solvents). Further attention, to their use to increase or maintain toughness is essential.

Clay based polymer nanocomposites research has mostly focused on smectite-based polymer composites.[14] They are particularly targeted to improve mechanical properties of thermoplastics such as heat distortion temperature, hardness, stiffness, and mold shrinkage.[12] However, natural clays have drawbacks such as variability in composition and color, difficulty in purification, poor reproducibility of the performance of polymer composites, crystallographic defects that prevent complete delamination.[15] Anionic clays such as layered double hydroxides (LDHs) are a potential alternative for the preparation of polymer composites. LDHs are hydrotalcite analogs also referred to as hydrotalcite-like compounds. They possess a brucite-like structure ($Mg(OH)_2$) where the divalent cations are isomorphously replaced by trivalent ones resulting in an overall positive charge, which is balanced by the presence of exchangeable anions. LDHs have a generic formula shown below.[16–19]

$$\left[M^{2+}_{(1-x)}M^{3+}_{x}(OH)_2\right]^{x+}A^{n-}_{(x/n)}\cdot mH_2O$$

Where M^{2+} is Mg, Zn, Ni, Co, Ca, Mn, etc.; M^{3+} is Al, Cr, Fe, Mn, Co, V, etc., and A^{n-} is CO_3^{2-}, Cl^-, NO_3^-, etc.

LDHs have advantages such as low incidence of impurities, reproducibility and uniform size control since they are synthetic. Moreover, a wide variety of metal species and mole ratio compositions can be prepared. LDHs however have a high charge density (0.031–0.041 equivalents per $Å^2$), hence the electrostatic interaction between the layers is very strong.[20,21] This aspect renders them unattractive as they would not easily delaminate or exfoliate in polymeric matrices. However, this "handicap" may be counteracted by intercalation. Intercalation is achieved by the insertion of exchangeable organic anions, hence reducing the solid–solid interaction within the clay layers. This is essential as the van der Waals interaction between solid surfaces decreases with the square of the separating distance.[15] Insertion of anions such as long chain carboxylic acids such as palmitic acid functionalizes the clay by converting the hydrophilic nature of the interlayer into a hydrophobic one. It also improves the compatibility of the clay with the polymer matrices in the preparation of polymer–clay nanocomposites.[15] A high surface coverage of the LDHs by surfactants would render them easily dispersible in the polymer, particularly a hydrophobic matrix.

Because of widespread increase of environmental concerns on the use of polymers, biocompatible, and biodegradable synthetic polymers such as aliphatic polyesters based on lactone and lactides,[22,23] are receiving growing attention. Polycaprolactone (PCL) is an aliphatic polyester, prepared through a ring-opening polymerization of the cyclic monomer ε-caprolactone.[24] It has applications in packaging and drug delivery. However, like most biopolymers, PCL suffers from poor mechanical performance and barrier properties (gases and water vapor). The mentioned shortcomings limit the use of PCL in the industry.[25] Hence, mineral fillers may be added to improve some of these properties.

Generally LDHs based polymer composites are prepared by three main techniques that is melt blending, solution intercalation and *in situ* polymerization. LDH-PCL composites have specifically been prepared by high energy ball milling (HEBM),[26,27] melt-blending,[28] and electrospinning.[29,30] Research to date has focused mainly on LDH-PCL composites for drug delivery aspects,[27,29,30] morphology, and dispersion of systems.[28] Sorrentino et al.[26] reported mechanical properties (modulus, stress at yield point, strain at break point, and stress at break value) improvement in LDH-PCL composite up to 2.8 wt %; however, the polymer suffered molecular weight reduction. Meanwhile, to the best of our knowledge a holistic study of the properties exhibited by LDH-PCL composites has not been reported. Furthermore, in view of environmental concerns, the LDH-PCL composite system in this study potentially offers benefits in its preparation as it is melt blended and thus no solvents are used. The matrix is biodegradable and palmitic acid is an environmental friendly surfactant. Mg-Al LDHs was modified and fully characterized. The study reports bilayer intercalated palmitic acid in Mg-Al layered double hydroxides above the normal anionic exchange capacity (AEC) and its dispersion in a low melting PCL matrix. A correlation of mechanical and thermal properties as well as changes crystallization morphologies is established.

EXPERIMENTAL

Materials

Materials used in the study are given in Table I. Materials were used as received from the supplier without further modification.

Preparation of LDH-Palmitate

Twenty grams of LDH-CO_3 was modified through a one-pot synthesis using palmitic acid. Forty grams of the Tween 60 was dispersed in 1.5 L of preheated distilled water at 70°C. The nonionic surfactant (Tween 60) was used to emulsify the palmitic acid. Three and half times the AEC of palmitic acid (0.288 mol) was used in the intercalation process. The addition of palmitic acid was divided into three portions added in three successive days to facilitate a high degree of self-assembly. The specimen was prepared at 70°C. Ammonia solution was added to maintain the pH of the reaction between 9 and 10. The specimen was recovered by centrifugation and washed four times with distilled water; once with both ethanol and acetone.

Preparation of LDH-PCL Composites

A Haake Rheomix internal mixer with two roller rotor was used in the preparation of LDH–PCL composites. The PCL and LDH-palmitate were pretreated at 55°C for 24 h prior melt-blending. The composite was prepared at 120°C for 10 min. 0, 1, 5, and 10 wt % composites were prepared. The melt-blended specimens were compression molded at 120°C in a Carver laboratory press.

Characterization

An Auriga field emission scanning electron microscope (FE-SEM, Zeiss, Germany) with a Gemini column, was used to view the LDHs powders and fractured surfaces of impact strength specimens. The composites fractured surfaces examined were obtained from Charpy impact tests. The specimens were mounted on the specimen holder and coated three times with carbon using the auto coating unit EMITECH K950X (Quorum Technologies, UK).

Table I. Materials and Supplier Information

Material	Supplier	Comment
PCL	Sigma Aldrich-South Africa	M_{wav}= 70-90kg/mol by GPC Lot No. MKBK2903V
LDH-CO_3	Nkomazi Holdings-South Africa	AEC of 400 meq/100 g
Palmitic acid	Sigma Aldrich-South Africa	Purity ≥80%
Ammonia solution	Sigma Aldrich-South Africa	28% NH_3 in H_2O
Tween 60 (polyoxyethylene-20-sorbitan monostearate)	Sigma Aldrich-South Africa	-

The LDH dispersion in PCL matrix was directly visualized using high resolution TEM (HRTEM). Specimens were prepared from compression molded LDH-PCL composites. Sections from all composite samples were obtained from Leica (Austria) EM UC6 cryo-ultramicrotome set at −120°C and a cutting speed of 0.08 mm/s using a diatome 35° diamond knife (Diatome, Switzerland). Sections with a nominal thickness of 90 nm were mounted on a 300 mesh copper grid and viewed. Calibrated images were captured with JEOL2100 HRTEM (JEOL, Japan) set at an operating voltage of 200 kV and using a Gatan Ultra scan camera and Digital Micrograph software (Gatan, USA).

Phase identification was carried out by XRD analysis on a PAN analytical X-pert Pro powder diffractometer (PANanalytical, the Netherlands). The instrument features variable divergence and receiving slits and an X'celerator detector using Fe-filtered Cu K-α radiation (0.154184 nm). X'Pert High Score Plus software was used for data manipulation. Temperature-resolved XRD traces were obtained using an Anton Paar HTK 16 heating chamber with a Pt heating strip. Scans were measured between $2\theta = 1°$ and 40° in a temperature range of 40 to 200°C in intervals of 10°C with a waiting time of 1 min and measurement time of 6 min/scan. Si (Aldrich 99% pure) was added to the samples so that the data could be corrected for sample displacement using X'Pert High Score plus software.

FTIR spectra were recorded on a Perkin Elmer 100 Spectrophotometer (Perkin Elmer, USA) with a MIRacle ATR attachment with diamond Zn/Se plate. A small amount of specimen was pressed onto the Zn/Se plate. The reported spectra were obtained over the range 4000–650 cm^{-1} and represent an average of 16 scans at a resolution of 2 cm^{-1}.

Differential scanning calorimetry (DSC) data was collected from a TA instrument (Q2000, USA). Approximately 5–10 mg of specimen was placed in an aluminum pan. The specimen was heated from −20 to 120°C at a scan rate of 10°C/min and at a N_2 flow rate of 25 mL/min. The same conditions were maintained in the cooling ramp. Figure 5(b) presents DSC carried out on a 5–10 mg specimen heated from −20 to 150°C at a scan rate of 10°C/min; and at a N_2 flow rate of 25 mL/min. The specimens were run in triplicate.

Dynamic mechanical properties of neat PCL and its LDH-palmitate containing composites were carried out on a Perkin Elmer DMA 8000 dynamic mechanical analyzer (DMA) (Perkin Elmer, USA) using the dual cantilever bending mode. The applied frequency was 1 Hz. The applied strain amplitude was 0.05% and specimens were run in duplicates. The temperature was scanned at 2°C/min from −100 to 50°C.

Tensile testing was carried out on an Instron 5966 tester (Instron, USA) according to ASTM D 638 using Type IV specimens obtained from compression molding. The specimens were analyzed without further annealing. Five specimens were tested for each composite. Charpy impact testing was carried out on a CEAST (Italy) Resil Impactor using the 15 J hammer, on single notched specimen prepared on an CEAST (Italy) Automatic Notchvis Plus.

Water vapor transmission rate of the neat PCL and LDH-palmitate containing composites was measured in a MOCON PERMATRAN-W® Model 3/33 (MOCON, USA). The test area of the compression-molded films with a thickness of 0.1 ± 0.05 mm was reduced to 5 cm^2 using aluminum masks. Permeability cells were flushed using nitrogen and specimens were conditioned for 24 h prior testing. The temperature was fixed at 37.8°C and relative humidity of 13.9%. The specimens were run until a steady-state was reached.

Atomic force microscopy (AFM) was carried on cryo-microtomed sections with a nominal thickness of 100–150 nm placed on a silicon wafer using on a multimode Nanoscope IVa AFM (Bruker Digital Instruments, USA). *In situ* studies were carried out on tapping mode and equipped with a high-temperature heater accessory. Images were captured after heating to 70°C and then cooled to 36°C. The examined area was 30×30 μm^2.

RESULTS AND DISCUSSION

The LDH-CO_3 prior modification had a platy morphology comprising of mostly subhedral crystals. The average lateral size of the particles being a couple of nanometers to micron size (Figure 1). The intercalated product i.e., LDH-palmitate, had similar subhedral platelets that were substantially larger in size than the pristine LDH. This suggests that the modification process was accompanied by dissolution and recrystallisation reactions resulting in morphological changes.[19]

Figure 2 shows diffractograms of the LDH-CO_3 and its palmitate modified form. LDH-CO_3 has peaks positioned at 2 theta values of 13.5° and 27.2°. However, in the LDH-palmitate there is a distinct shift of characteristic LDH peaks to lower 2 theta

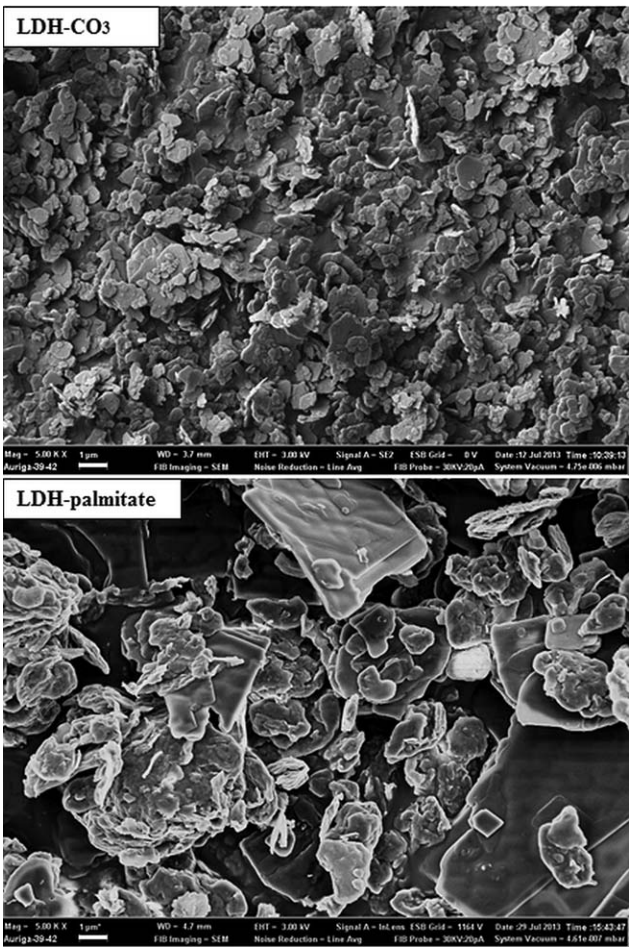

Figure 1. SEM images of LDH-CO_3 and LDH-palmitate.

values, which is indicative of interlayer expansion. The d-spacing increased from 0.76 to 4.71 nm. This degree of interlayer expansion suggests a bilayer type of self-assembly within the gallery space. The intercalated palmitic acid anions are envisaged to have a tilt angle of 62°, based on the calculation in the equation given below.[31,32]

$$d = 1.48 + 0.26(n-2)\sin \quad (1)$$

where d is the d-spacing, n is the carbon number in the palmitate chain, θ is the slant angle of the intercalated palmitic acid anions.

The degree of layer separation is governed by the dimensions and functional group of the anions intercalated. Other factors include the AEC level of the anions intercalated, size, orientation, and interaction with the hydroxyl lattice.[33] It is evident from the diffractogram that the LDH-palmitate is highly ordered due to the sharp and symmetric peaks. However, there are palmitic acid impurities in the case of LDH-palmitate demonstrated by the existence of a shoulder next to the primary peak. This further substantiates the claim of cointercalation of excess fatty acid and this second layer of undissociated acid will lead in greater d-spacings.[33–35] Additionally, in the thermogravimetric data the degree of carboxylate intercalation was found to be 2.24, with a percentage organic of 73%. Nhlapo et al.[36] calculated the theoretical possible amount to be 2.39 times the AEC for close-packed carboxylate chains. It is evident that the degree of intercalation occurs at a higher level than the AEC expected for LDHs, implying that the excess exists as un-ionized fatty acids.

FTIR spectra of LDH-CO_3, LDH-palmitate, and palmitic acid are presented in Figure 3 and corroborate the XRD findings. Figure 3(b) is a zoom-in of the region 1800–1200 cm^{-1}. FTIR helps in the identification of intercalated species and their state within the LDH-interlayer. With regards to the LDH-CO_3, the broad band in the range of 3400–3500 cm^{-1} is assigned to υ_{OH} OH···HOH vibrations. The shoulder at 3000–3100 cm^{-1} is attributed to the OH vibrations of hydroxyl groups' co-ordinated to the interlayer carbonate $OH{\cdot}CO_3^{2-}$ through hydrogen bonding. A bending vibration (δH_2O) from the interlayer water is observed at 1600–1650 cm^{-1}. Carbonate anion peaks are observed at 850–880 cm^{-1} (υ_2), 1350–1380 cm^{-1} (υ_3), and 670–690 cm^{-1} (υ_4). The intensity of the (υ_3) peak gives an indication of the degree of exchange of the carbonate anion by palmitate anions, of which in this case significantly reduced. LDH-palmitate peaks in the regions 2956, 2915, and 2848 cm^{-1} are attributed to CH_2 symmetric and asymmetric stretching modes. The $\upsilon_{as}CH_2$ band is observed at a low wavenumber (2915 cm^{-1}), which is an indication of good conformational order within the layers.[34]A bending vibration of the intercalated water $\delta(\upsilon H_2O)$ is observed at 1636 cm^{-1}; however, it overlaps with the COO^-H^+ vibration. Bands at 1586, 1541, 1466, 1429, and 1415 cm^{-1} are vibrations due to carboxylic group. The different bands are indicative of the diverse states of the carboxylic present within the interlayer. These include COO^-H^+ (OH) vibration at 1586 and 1541 cm^{-1}, whilst the 1429 and 1415 cm^{-1} are attributed to the undissociated palmitic acid. A medium peak around 1466 cm^{-1} is assigned to CH_2 bending of the carboxylic acid chain.[36] The summation of peaks observed is confirmation of the presence of both palmitate ions and palmitic acid within the interlayer.

Figure 4 shows X-ray diffactograms of the different composites. In the LDH-palmitate filled polymer systems the primary peaks

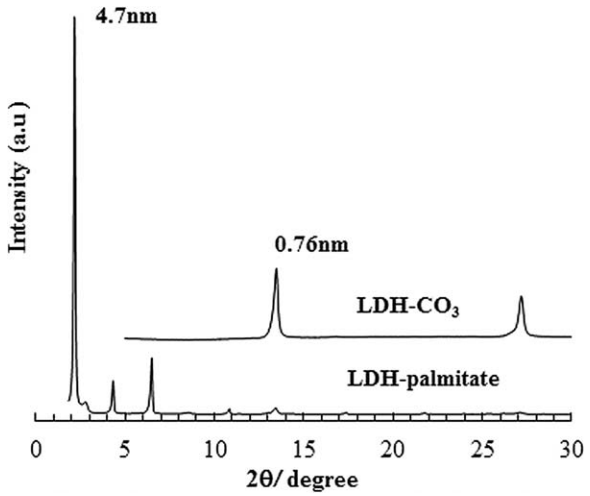

Figure 2. XRD diffractogram of LDH-CO_3 and LDH-palmitate.

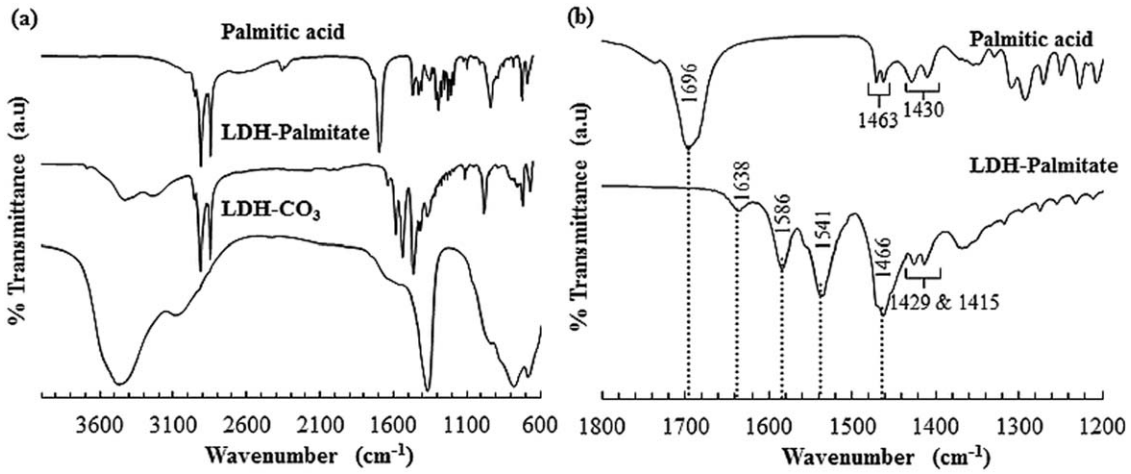

Figure 3. FTIR spectra of LDH-CO_3, LDH-palmitate, and palmitic acid.

disappear for low filled systems, i.e., 1 wt %. This could be an indication of highly dispersed (delaminated) polymer systems. However, above 5 wt % loading a residual peak at 3.75 (2 theta) is observed, this is consistent with a monolayer intercalated LDH-palmitate with a d-spacing of 2.36 nm, which is similar to that obtained by Borja and Dutta, 1992 (2.37 nm).[37] The peak intensity increases with increase in filler content, this could be a dilution effect. Intercalated species have been observed to demonstrate thermotropic behavior that is followed by changes in the d-spacing due expulsion of water and free fatty acid molecules.[34,36,38] This is clearly demonstrated in Figure 5(a). The multiplicity of endothermic peaks in Figure 5(b) is indicative of various components present in the specimen. It is probable that the bilayer LDH-palmitate is composed of randomly interstratified clay. It is clear that as temperature increases the d-spacing decreases. The red triangles indicate the temperature at which there is an emergence of successive phase with a lower d-spacing. The layers collapse to a spacing of 2.8 nm at 160°C. The disparity between the spacing observed for the composite system and the heated LDH-palmitate is due to shear action during processing resulting in a much lower d-spacing. However, the use of XRD as a standalone technique may give a misrepresentation on the dispersity of the filler; hence TEM is used to obtain visual evidence.

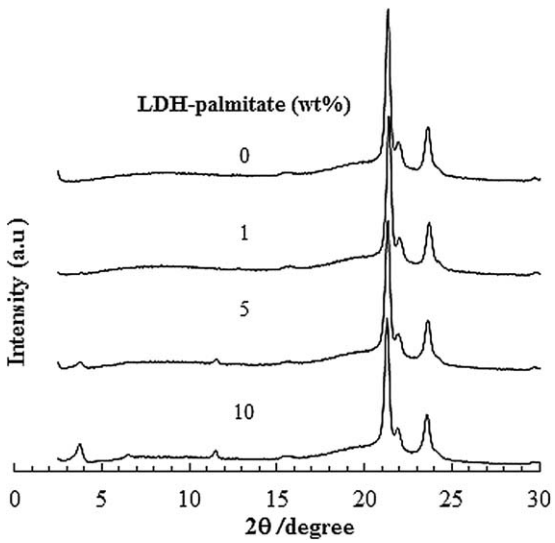

Figure 4. XRD diffractogram of LDH-PCL composites.

The TEM images (Figure 6) present the dispersion of LDH in the polymer matrix. Low magnification images are not presented as they were not visible due to the fine dispersion of the LDH-palmitate within the polymer matrix. Some delaminated sheets are observed at a nanoscale level. The nanometer dispersion is desirable as it plays a significant role in directing morphology and introducing new energy-dissipation mechanisms in toughening nanocomposites.[39] Moyo et al.[38] also reported that highly dispersed and randomly oriented nanosized clay platelets promoted extensive internal microcavitation during impact loading. However, as the amount of filler increases, tactiods become more prominent especially in the 10 wt % filler loaded composite. The presence of tactoids is an indication that there is some form of registry of clay layers within the 5 and 10 wt % composites, which is detected in XRD as a residual peak of monolayer LDH-palmitate. The clay platelets appear to be smaller in size, which may be attributed to mechanical fracture during melt-blending. LDHs are composed of three atomic layers as compared to the cationic counterparts with 6–7 layers. Hence, the former is more susceptible to deformation or breakage than the latter during processing.

Mechanical properties for the neat PCL and derivative composites are shown in Table II. Increase in the modulus is observed indicating the reinforcement property of the LDH-palmitate. The 10 wt % composite showed the greatest increase in the modulus this may be related to the higher filler loading. With regards to this particular composite, a high level of tactoids is observed in the TEM images and such morphology in combination with delaminated regions will also result in a high modulus. The 5 wt % has a lower modulus as compared to the other specimens; this may be explained by a reduction in crystallite sizes as will be discussed later in the crystal morphology. A decrease in the tensile strength property is also observed as the filler content increases. It is evident in the TEM micrographs that the highly filled specimen (10 wt %) has a lot of tactoids.

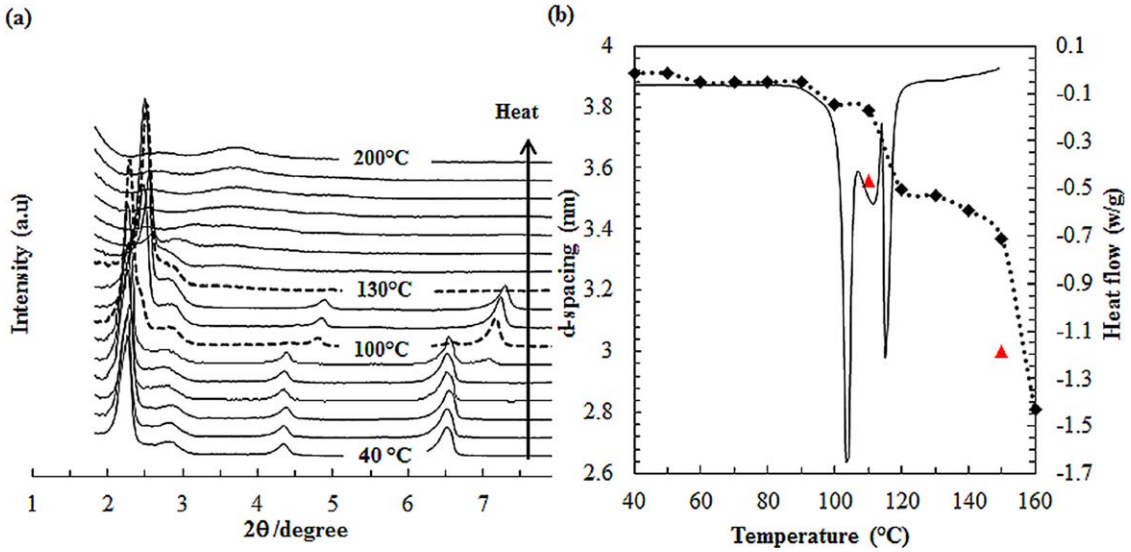

Figure 5. Thermotropic behaviour of LDH-palmitate (a) temperature scan XRD and (b) change in d-spacing as compared to thermal event from DSC. [Color figure can be viewed in the online issue, which is available at wileyonlinelibrary.com.]

These tactoids may act as stress concentrations resulting in poor tensile strength. Nanocomposite mechanical performance is strongly dependent on the degree of delamination; hence, it may be inferred that the dispersion in the 10 wt % is not optimal.[14] The strength of a matrix is dependent on the size and distribution of defects or flaws in the specimen; which in turn determines the degree of load it can withstand prior to failure.

Anomalous impact strength is obtained for the 5 wt % composite, where a 65% increment in strength is observed as compared to the neat polymer. The LDH-palmitate acts as an impact strength modifier in this composite system. Polymer toughening modifiers have been proposed to alter the stress state in the material around the particles and induce extensive plastic deformation, e.g., multiple crazing, shear banding, crazing with shear yielding and debonding of the inorganic filler particles.[11] These deformations constitute a range of different energy-absorption mechanisms such as increase in the internal structure, hence preventing premature fracture. Figure 7 shows a SEM micrograph of the fracture surface of the impact strength specimen. The matrix is characterized by extensive areas with microcavitation, which may be an indication of the polymer toughening mechanism. This type of morphology is observed mainly in the 5 wt % composition. In this system the LDH-palmitate can be considered as a nucleation site for microvoid formation. Figure 7(b,c) shows a particle that seems to have been dislodge from the matrix and its corresponding energy dispersive X-ray (EDX) map, respectively. An area with microvoids is left behind. An analysis of variance was carried out separately for each test that is modulus, impact, tensile strength. etc. The results are statistically different with a confidence level greater than 95% across the sample groupings. The associated *p*-values in Table II are

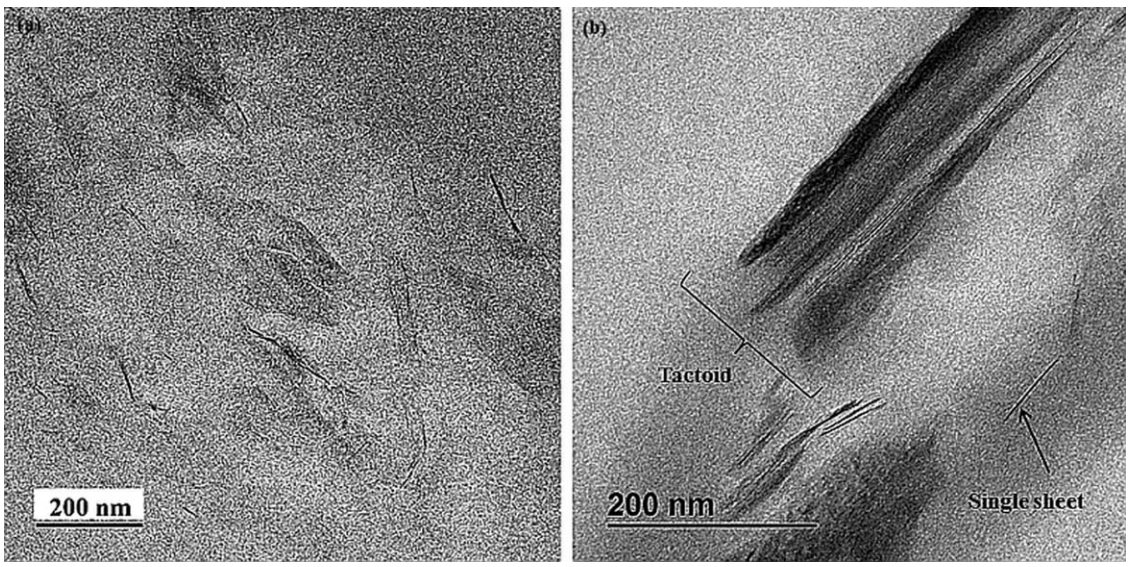

Figure 6. TEM images for the LDH-PCL composites (a) 5 wt % and (b) 10 wt %.

Table II. Mechanical Properties and Water Vapor Transmission of Neat PCL and Respective Composites

LDH-palmitate wt %	Modulus (MPa)	Tensile strength (MPa)	Impact resistance (kJ/m^{-2})	Water transmission rate (g/[m^2/day])[a]	Permeation rate (g/mm/[m^2/day][a]
0	410 ± 24	67 ± 9	192 ± 45	26 ± 1	102 ± 3
1	438 ± 25	61 ± 11	172 ± 17	15 ± 5	64 ± 21
5	425 ± 28	55 ± 1	316 ± 80	13 ± 3	52 ± 12
10	458 ± 23	43 ± 3	170 ± 22	20 ± 3	78 ± 10
p value	0.051	0.0003	0.0006	0.0005	0.0009

[a] Temperature 37.8°C, 13.9% relative humidity.

statistically highly significant thus suggesting that mechanical properties are affected by the weight of the LDH-palmitate in the composite.

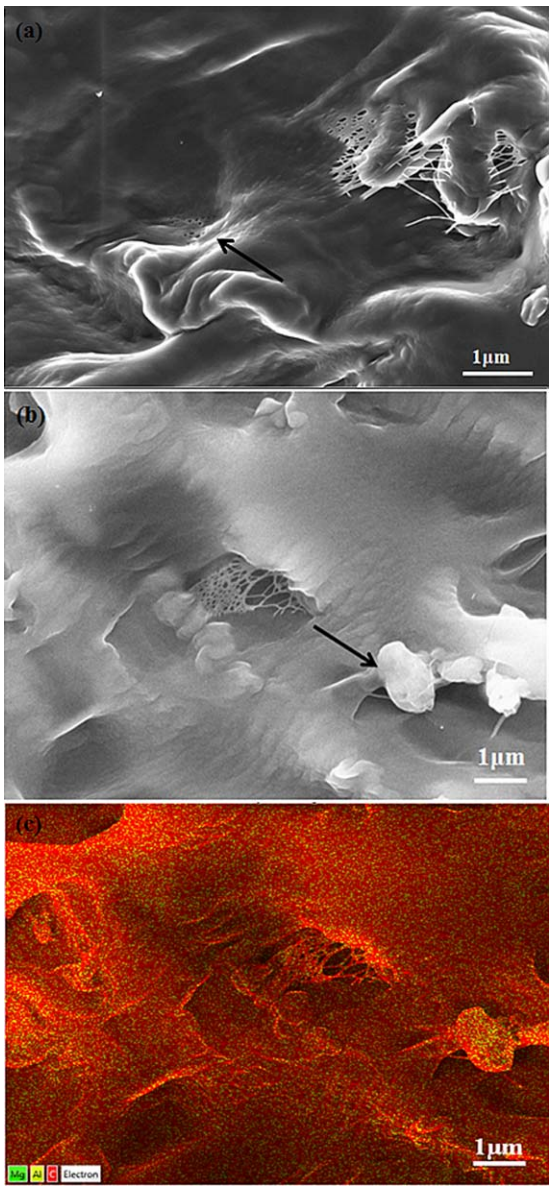

Figure 7. Microcavitation observed throughout the Charpy impact strength specimen (5 wt % LDH-PCL). [Color figure can be viewed in the online issue, which is available at wileyonlinelibrary.com.]

The water vapor transmission rate (Table II) decreased for all the composite specimens as compared to neat specimen, which is likely due to the presence ordering of filler particles in such a way that the diffusion path is torturous and impervious to water molecules. The impervious aspect may also be supported by the presence of excess fatty acids exuded in the polymer matrix as demonstrated in Figures 4 and 5. Exuded fatty acid is likely to increase the hydrophobic characteristics of the polymer therefore hindering the passage of water molecules. The improvement in the water vapor barrier properties makes the filler potentially attractive for use in the food packing application. Hydrolysis of the PCL matrix is dependent on the transport of water from the surface to the bulk of the material. Hence, a reduction in water vapor transmittance rate (WVTR) is an added benefit for modifying degradation rates.[25]

Dynamic mechanical properties are shown in Figure 8. The reinforcement ability of LDHs is further demonstrated by a higher storage modulus (E') for the composites as compared to the neat polymer in the glassy region [Figure 8(a)]. It is notable that the 5 wt % composite is higher than all the other compositions in the rubbery region, which may be attributed to a favorable dispersion and interaction with the matrix. This observation may also be explained as continued reinforcement or extended intercalation at higher temperatures. It is evident from the loss modulus data [Figure 8(b)] that motion of polymer chain segments begins at a lower glass transition temperature. This is an indication of a plasticizing effect of the LDH-palmitate. As the filler content increases the fluidity of the matrix also increases. This could be related to the excess fatty acids exuded into the matrix during processing; in this instance the amount of free fatty acid available in the composite will be proportional to the filler added hence a greater shift to left is observed in the higher filler loaded specimens. Lowering of the glass transition temperature suggests increased polymer chain mobility or flexibility and possible increase in free volume. These thermomechanical changes are typical of an impact strength resilient material, as demonstrated by the 5 wt % composite.

Table III presents DSC data of melting and crystallization of PCL and respective composites. The data discussed pertain to those obtained from the second heating and first cooling. The onset of melting and T_m remain unchanged in all specimen with the exception of the enthalpy of fusion. The enthalpy of fusion increased slightly for the 10 wt % LDH-palmitate

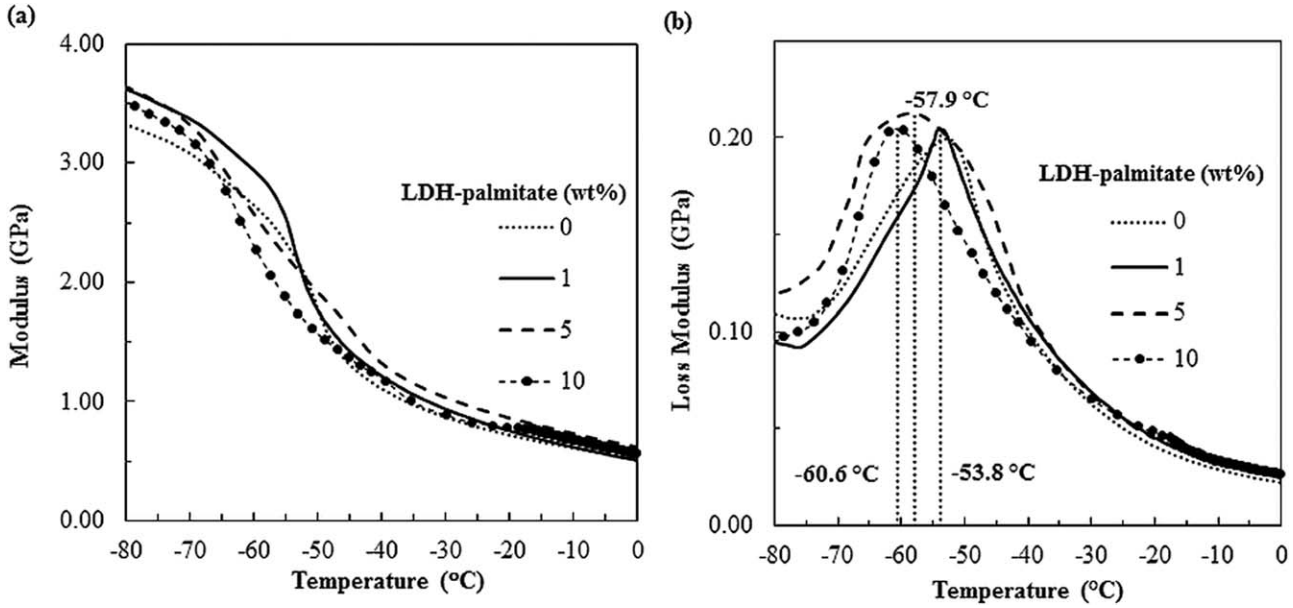

Figure 8. Dynamic mechanical properties of neat PCL and LDH-PCL composites (1 Hz).

loading. Increase in the heat of fusion is generally an indication of larger crystallites forming. The onset of crystallization and crystallization peak shifts to higher temperature for the filled composites and is more evident in higher composition of filler i.e., 5 and 10 wt % (Figure 9). This may be attributed to the LDH-palmitate particles acting as heterogeneous nucleation sites in the polymer matrix.

Crystallite morphology of semicrystalline polymers is normally affected by the presence of particulate filler. To further study the morphology of the LDH-palmitate composites, AFM was employed. Figure 10 shows AFM 30 × 30 μm^2 height and amplitude micrograph of the neat PCL and composite systems. The AFM micrographs of the neat PCL had large asymmetric crystals with an average diameter of 18 ± 2 μm [Figure 10(a)]. In the 5 wt % composite the crystals appear smaller in size and measured 25% less in diameter as compared to the neat polymer [Figure 10(b)]. The lamellae of the crystals in the 5 wt % appear to be thinner as compared to the neat and 10 wt % composite. Shah et al.[39] found that incorporation of nanoclay resulted in increase in toughness attributed to reduction in spherulite size and formation of more mobile crystallites. In their study they found a dramatic increase up to 700% higher than the neat polymer in toughness and 70% higher in elongation at break for polyvinylidene fluoride nanocomposite with 5 wt % organo-clay based on the area under the tensile stress–strain curve. The enhanced toughness was attributed to a transition from α-spherulites to thin fiber-like β-crystallites, which reoriented in the strain field. This could help explain the anomalous toughness observed in the 5 wt % composite, the composite exhibits a reduction in crystallite size and a more "fluid" matrix is observed [Figure 8(b) and 10]. Chen et al.[40] corroborate that the formation of more ductile crystallite phases leads to improved toughness. Additionally, Gersappe[41] proposed that improved mechanical properties result more from the mobility of particles during deformation than from the stiffening effect of the matrix by the reinforcement. The 10 wt % LDH-palmitate polymer composite exhibited areas with large irregular lozenge-shaped crystallites as seen in Figure 10(c′). These large crystallites and high level of tactoids within the matrix presumably act as stress concentrations within the matrix when an external load is applied; hence the material undergoes premature failure. It is clear from the 10 wt % composite images that the LDH-palmitate is mostly segregated to the areas where the spherulites impinge. This may also works to the detriment of mechanical properties.

Although the LDH-palmitate appears to influence some attractive properties, it is not as rigid as layered silicates, hence modest increases in modulus are observed. Moreover, the LDHs platelets are fragile and are prone to fracture during processing resulting in sheets with a smaller aspect ratio. Organo-LDHs

Table III. DSC Data of Melting and Crystallisation of PCL and Respective Derivatives

LDH-palmitate (wt %)	Onset of melting (°C)	T_m (°C)	ΔH_m (J/g)	Onset of crystallization (°C)	T_c (°C)	ΔH_c (J/g)
0	54	56 ± 0.1	58 ± 1.3	35 ± 0.1	33 ± 0.1	57 ± 2.4
1	54	56 ± 0.1	58 ± 1.1	35	33 ± 0.1	55 ± 0.3
5	54	56 ± 0.1	59	36	34	56 ± 1. 5
10	54	56 ± 0.1	63 ± 7.3	34	34 ± 0.1	57 ± 5.6

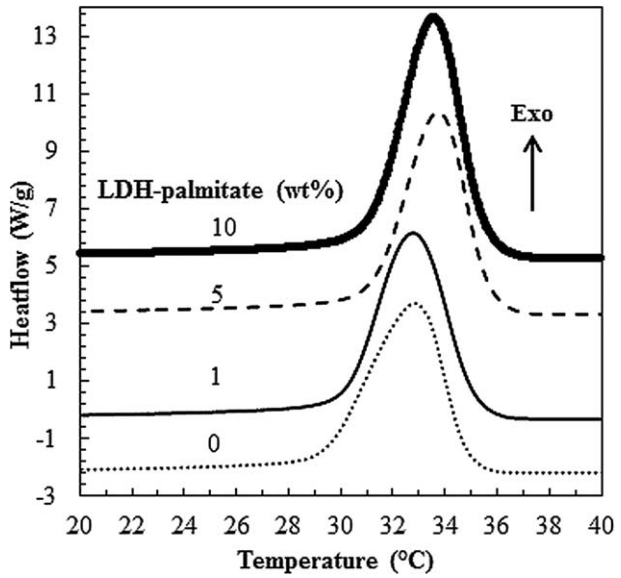

Figure 9. DSC cooling run of PCL and derivative LDH-PCL composites.

that do not show thermotropic behavior at typical polymer processing temperature may be studied so as to minimize the effects of the exuded surfactants on the matrix. Further study on the reduction of the water vapor transmission rate would be worthwhile to further reduce vapor transmission particularly for food packaging applications.

CONCLUSION

Results from the present study suggest that palpitate ions and molecules cointercalate to achieve a tightly packed bilayer within the LDHs interlayer. Melt blending of the bilayer LDHs precursor with the polymer resulted in a composite system with residual monolayer peaks observed in the 5 and 10 wt % composites, respectively. The internal structure of the composite systems prepared was predominately in the nanoscale range as determined through XRD and TEM characterization. However, at higher filler loadings tactoids were observed, particularly in the 10 wt % composite. Improvement in impact strength for the 5 wt % composite is attributed to the combination of microcavitation, crystallite size changes as well as a more flexible polymer matrix. These properties work together as energy dissipation mechanisms preventing premature fracture. It is evident that the LDH-palmitate plays a pivotal role in redirecting morphology and introducing new energy-dissipation mechanisms for polymer toughening. A reduction in the water vapor transmission rate is also observed. The filler shows promising

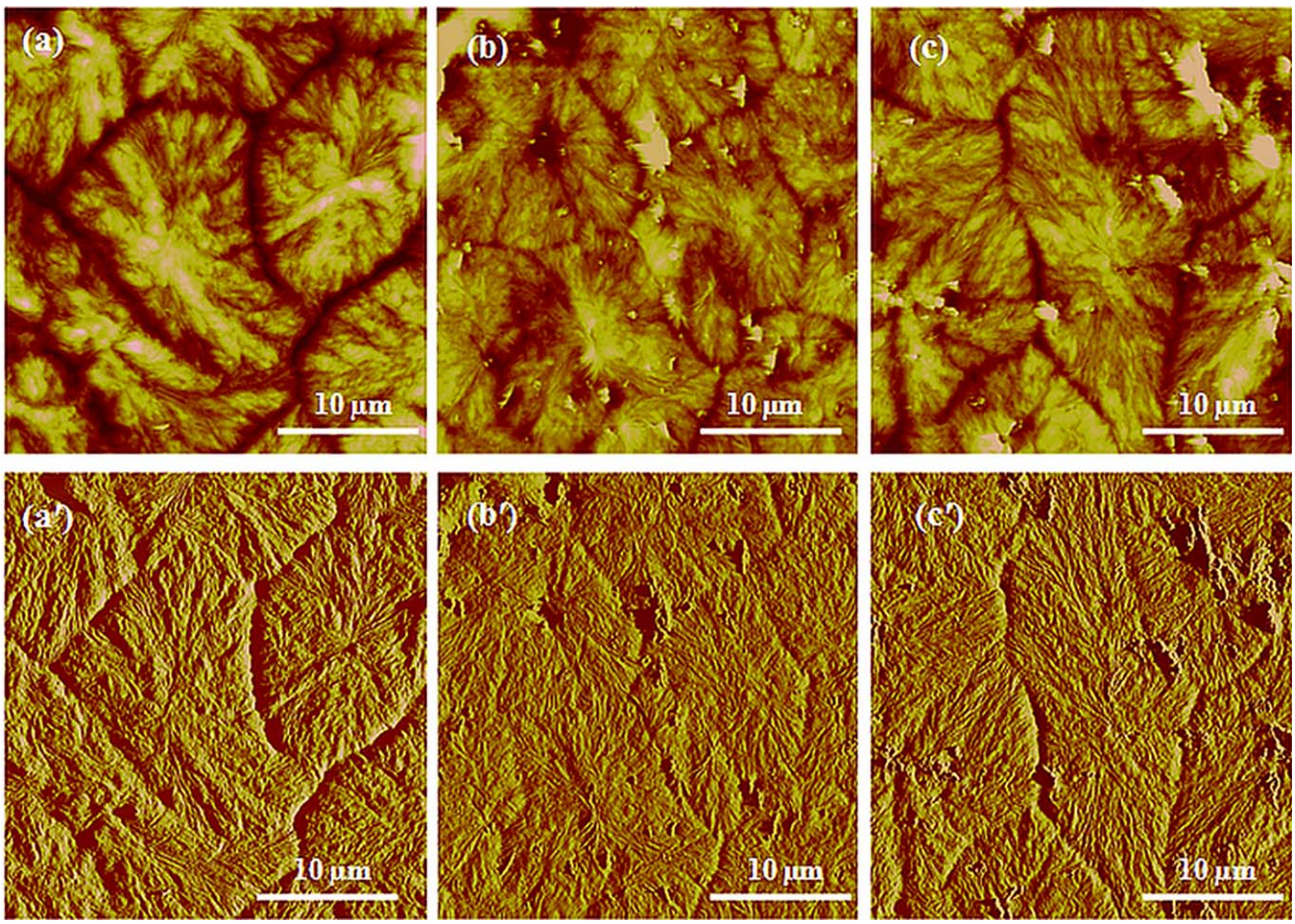

Figure 10. AFM height and amplitude micrographs of (a) neat polymer and (b) 5 wt %, and (c) 10 wt % LDH-PCL composite and amplitude micrographs for a′, b′, and c′, respectively. [Color figure can be viewed in the online issue, which is available at wileyonlinelibrary.com.]

use as a multifunctional additive in polymeric matrices able to achieve stiffness whilst retaining/improving impact strength.

ACKNOWLEDGMENTS

The authors would like to thank the Department of Science and Technology, the Council for Scientific and Industrial Research, and the National Research Foundation, South Africa for financial support.

REFERENCES

1. Kim, G. M.; Michler, G. H. *Polymer.* **1998**, *39*, 5689.
2. Galeski, A. *Prog. Polym. Sci.* **2003**, *28*, 1643.
3. Gao, F. *Mater. Today.* **2004**, *7*, 50.
4. Moniruzzaman, M.; Winey, K. I. *Macromolecules.* **2006**, *39*, 5194.
5. Huang, J.; He, C.; Liu, X.; Xu, J.; Tay, C. S. S.; Chow, S. Y. *Polymer.* **2005**,*46*, 7018.
6. Lui, Z.; Ma, R.; Osada, M.; Iyi, N.; Ebina, Y.; Takada, K.; Sasaki, T. *J. Am. Chem. Soc.* **2006**, *128*, 4872.
7. Kalaitzidou, K.; Fukushima, H.; Drzal, L. T. *Carbon.* **2007**, *45*, 1446.
8. Althues, H.; Henle, J.; Kaskel, S. *Chem. Soc. Rev.* **2007**, *36*, 1454.
9. George, J.; Sreekala, M. S.; Thomas, S. *Polym. Eng. Sci.* **2001**, *41*, 1471.
10. Vaia, R.; Wagner, H. *Mater. Today.* **2004**, *7*, 32.
11. Zuiderduin, W. C. J.; Westzaan, C.; Huétink, J.; Gaymans, R. *J. Polymer.* **2003**, *44*, 261.
12. Chan, C.-M.; Wu, J.; Li, J.-X.; Cheung, Y.-K. *Polymer.* **2002**, *43*, 2981.
13. Cotterell, B.; Chia, J. Y. H.; Kbaieb, K. *Eng. Fract. Mech.* **2007**, *74*, 1054.
14. Ray, S. S.; Okamoto, M. *Prog. Polym. Sci.* **2003**, *28*, 1539.
15. Utracki, L. A. Clay-Containing Polymeric Nanocomposites, Vol. 1.; Rapra Technology: Shrewsbury, UK, **2004**, p 456.
16. Brindley, G. W.; Kikkawa, S. *Am. Mineral.*, **1979**, *64*, 836.
17. Miyata, S. *Clays Clay Miner.*, **1980**, *28*, 50.
18. Mascolo, G.; Marino, O. *Miner. Mag.*, **1980**, *43*, 619.
19. Cavani, F.; Trifirò, F.; Vaccari; A. *Catal. Today*, **1991**, *11*, 173.
20. Meyn, M.; Beneke, K.; Lagaly, G. *Inorg. Chem.* **1990**, *29*, 5201.
21. Carrado, K. A.; Xu, L. *Microporous Mesoporous Mater.* **1999**, *27*, 87.
22. Lepoittevin, B.; Devalckenaere, M.; Pantoustier, N.; Alexandre, M.; Kubies, D.; Calberg, C.; Jerome, R.; Dubois, P. *Polymer.* **2002**, *43*, 4017.
23. Ray, S. S. Environmentally Friendly Polymer Nanocomposites: Types, Processing and Properties. No. 44. Woodhead Publishing Series in Composite Science and Engineering: Sawston-Cambridge, **2013**, p 488.
24. Hutmacher, D. W.; Woodruff, M. A. *Prog. Polym. Sci.* **2010**, *35*, 1217.
25. Rhim, J.-W.; Park, H.-M.; Ha, C.-S. *Prog. Polym. Sci.* **2013**, *38*, 1629.
26. Sorrentino, A.; Gorrasia, G.; Tortora, M.; Vittoria, V.; Constantino, U.; Marmottini, F.; Padella, F. *Polymer.* **2005**, *46*, 1601.
27. Bugatti, V.; Gorrasi, G.; Montanari, F.; Nocchetti, M.; Tammaro, L.; Vittoria, V. *Appl. Clay Sci.* **2011**, *52*, 34.
28. Manhique, A.; Focke, W. W.; Leuteritz, A.; Madivate, M. *Mol. Cryst. Liq. Cryst.* **2012**, *556*, 114.
29. Miao, Y.-E.; Zhu, H.; Chen, D.; Wang, R.; Tjiu, W. W.; Liu, T. *J. Mater. Chem. Phys.* **2012**, *134*, 623.
30. Tamarro, L.; Costantino, U.; Bolognese, A.; Sammartio, G.; Marenzi, G.; Calignano, A.; Tet`e, S.; Mastrangelo, F.; Califano, L.; Vittoria, V. *Int. J. Antimicrob. Ag.* **2007**, *29*, 417.
31. Carlino, S. *Solid State Ionics.* **1997**, *98*, 73.
32. Xu, Z. P.; Braterman, P. *Appl. Clay Sci.* **2010**, *48*, 235.
33. Braterman, P. S.; Xu, Z. P.; Yarberry, F. In Handbook of Layered Materials; Auerbach, S. M.; Carrado, K. A.; Dutta, P. K., Eds.; CSC Press, Taylor & Francis Group: Boca Raton, **2004**, pp 373–449.
34. Focke, W. W.; Nhlapo, N. S.; Moyo, L.; Verryn, S. M. C. *Mol. Cryst. Liq. Cryst.* **2010**, *521*, 168.
35. Kuehn, T.; Poellmann H. *Clays Clay Miner.* **2010**, *58*, 596.
36. Nhlapo, N.; Motumi, T.; Landman, E.; Verryn, S. M. C.; Focke, W. W. *J. Mater. Sci.* **2008**, *43*, 1033.
37. Borja, M.; Dutta, P. K. *J. Phys. Chem.* **1992**, *96*, 5434.
38. Moyo, L.; Focke, W. W.; Labuschagne, F. J.; Heidenrich, D.; Radusch, H.-J. *Mater. Res. Bull.* **2013**, *48*, 1218.
39. Shah, D.; Maiti, P.; Gunn, E.; Schmidt, D. F.; Jiang, D. D.; Batt, C. A.; Giannelis, E. P. *Adv. Mater.* **2004**, *16*, 1173.
40. Chen, B.; Evans, J. R. G.; Greenwell, H. C.; Boulet, P.; Coveney, P. V.; Bowden, A. A.; Whiting, A. *Chem. Soc. Rev.* **2008**, *37*, 568.
41. Gersappe, D. *Phys. Rev. Lett.* **2002**, *89*, 58301.